Energy-Efficient Orchestration in Wireless Powered Internet of Things Infrastructures

Dimitrios Sikeridis, Eirini Eleni Tsiropoulou, *Member, IEEE*, Michael Devetsikiotis, *Fellow, IEEE*, and Symeon Papavassiliou, *Senior Member, IEEE*

***Abstract*—Multipurpose devices, capable of dynamically operating under various sensing modes, have emerged as a key element of the Internet of Things (IoT) ecosystem. In this paper, the holistic orchestration of an energy-efficient operational framework of such interconnected devices is investigated. A reinforcement learning technique is utilized enabling each IoT node, by acting as a learning automaton, to select a sensing operation mode in accordance with the IoT infrastructure's provider interests. Subsequently, a coalition formation among the nodes is realized, relying on their socio-physical relations, namely nodes' spatial proximity, energy availability, and mode correlations. The aforementioned operation is supported by a non-orthogonal multiple access wireless powered communication environment, where the nodes are able of harvesting energy from the base station. The energy efficiency of the overall system, is further improved by a utility-based optimal uplink transmission power control mechanism. The corresponding optimization problem is treated in a distributed manner as a non-cooperative game-theoretic problem, and the existence of a unique Nash equilibrium is shown, while the adoption of convex-based pricing in the utility leads to a more socially desirable Equilibrium point. The performance of the proposed approach is evaluated through modeling and simulation under several scenarios, and its superiority is demonstrated.**

***Index Terms*—Internet of Things, multipurpose devices, socio-physical ties, energy-efficiency, reinforcement learning.**

I. Introduction

THE INCORPORATION of Internet of Things (IoT) architectures into emerging smart ecosystems allows for a variety of innovative context-aware applications that rely on high-volumes of real-time sensed data. Until recently, the design of related systems was focusing on a single-use approach where a wireless sensor network (WSN) was deployed by a single owner, measuring a specific quantity, and supporting a single application [1]. However, the new model and scale of modern smart infrastructures where multiple applications operate simultaneously, requesting diverse data, makes this monolithic sensing application approach inefficient in terms of resource use [2]. Thus, under the new reality of continuously interconnected and sensor-packed devices that IoT introduces, both academia [3], [4] and industry [5] are turning to a new class of multipurpose devices. These sensing installations can operate under the supervision of an infrastructure owner who can after-profit distribute the sensed data to multiple interested users and IoT application frameworks.

Such a consideration is driven and further motivated by the emerging trend that "one size fits all" and allows software defined decision making approaches to govern and properly define the dynamic operation of multipurpose devices. This approach allows not only significant cost savings in terms of infrastructure installation and operation especially for IoT-enabled large scale deployments, but it further facilitates the support of a more dynamic, diverse, effective and cost-efficient operation paradigm for high-level applications with time and space varying requirements. Though the benefits obtained by adopting an operation model based on statistical and adaptive multiplexing at various levels, are multifaceted and follow naturally and inherently [6]–[8], there are several technical challenges that need to be addressed in order to allow its full realization and exploitation.

Specifically, the envisioned energy-efficient sensing in IoT, which is still considered as a research challenge [9], [10], can emerge as the outcome of adopting autonomous IoT devices with self-configuration characteristics. Investigated approaches include intelligent device-to-device (D2D) communications depending on context-awareness or intelligent routing [9], ecosystems of "Self-Organizing Things" [11], where IoT sensors are able to adopt self-optimization and self-healing mechanisms to save power by optimizing sleep mode periods, or holistic IoT architectures that utilize sleep interval control and adaptive wake-up signals for sensors towards energy efficiency in IoT middleware and hardware elements [10]. These self-organizing operations such as optimal sleep mode scheduling can significantly extend the battery life of IoT multi-sensor nodes (that sent data both periodically and in a trigger-based fashion), and are applicable in cases where the limited number of an IoT nodes' peripheral communication interfaces [12] allows for a single measurement extraction per transmission interval [10], [11].

Manuscript received July 16, 2018; revised September 9, 2018; accepted November 30, 2018. Date of publication December 7, 2018; date of current version May 16, 2019. The work of E. E. Tsiropoulou was supported in part by UNM Research Allocation Committee Award and in part by UNM Women in STEM Faculty Development Fund. The work of S. Papavassiliou was supported by NTUA-GSRT Research Award under Grant 67104700. The associate editor coordinating the review of this paper and approving it for publication was E. Ayanoglu. *(Corresponding author: Eirini Eleni Tsiropoulou.)*

D. Sikeridis, E. E. Tsiropoulou, and M. Devetsikiotis are with the Department of Electrical and Computer Engineering, University of New Mexico, Albuquerque, NM 87131 USA (e-mail: dsike@unm.edu; eirini@unm.edu; mdevets@unm.edu).

S. Papavassiliou is with the School of Electrical and Computer Engineering, National Technical University of Athens, 15780 Athens, Greece (e-mail: papavass@mail.ntua.gr).

Digital Object Identifier 10.1109/TGCN.2018.2885645

A. Related Work

In literature there are some preliminary research works that extend the notion of WSNs towards multipurpose ones. Chi *et al.* [3] introduce a reconfigurable smart sensor interface for industrial WSN in the IoT environment, where a complex programmable logic device is adopted in order to control the collection of different types of sensor data. A corresponding application of this approach is presented in [5] within the industrial IoT era. Steffan *et al.* [6] study a multi-application focused WSN architecture where a group of nodes (scopes) is specified supporting dynamic scope memberships and introducing a routing level able to maintain routing trees among members. That way the nodes form an ad-hoc multi-hop WSN resilient to link losses, and are able to collect data by assigning node subsets to specific applications. Sarakis *et al.* [8] introduce the concept of virtual sensor networking, which decouples the physical sensor deployment from the applications that run on top of it, thus providing the enhanced flexibility to the infrastructure owner to provide new services beyond to the scope of the original deployment. A detailed survey analysis is presented in [7] regarding the virtual sensor networking and the multi-sensing capabilities of the devices.

In addition to the multipurpose and multi-sensing capabilities of the devices, the energy efficient operation of the latter within the heterogeneous IoT arena arises as a major research challenge [13]. Recent research approaches aim to extend the energy availability of IoT environments through a variety of approaches that include the use of Wireless Powered Communication (WPC) techniques [14], social-aware clustering [15], and optimal resource allocation strategies for the battery-constrained IoT devices [16]. Zewde and Gursoy [17] investigate the performance of a non-orthogonal multiple access (NOMA)-based wireless network that utilizes WPC for the devices following a harvest-then-transmit protocol. The focus is on maximizing the system's energy efficiency through resource allocation strategies developed for the case of asynchronous and half-duplex transmissions. Tsiropoulou *et al.* [18] propose a low-complexity coalition formation mechanism among the IoT connected devices based on the Chinese Restaurant Process (CRP), while the devices harvest energy from the RF signals using the WPC technique. In [19] a framework for data dissemination using D2D communications is presented, considering a social-based model that captures and exploits users' social relationships within the community to improve dissemination efficiency. Similarly, the work in [20] focuses on a NarrowBand-IoT (NB-IoT) OFDMA-based environment and presents a social-aware D2D-enabled relay selection mechanism formulated as a double auction problem for data uploading towards a base station. In [15], the problem of interest, energy and physical-aware coalition formation and resource management in smart IoT applications is studied towards improving devices' energy efficient communication. Finally, in [21], a data-centric clustering is introduced in a resource-constrained IoT environment by prioritizing the quality of overall data over the performance of individual devices.

B. Contributions and Outline

The key contributions of our research work that differentiate it from the rest of the literature body [22], are summarized as follows:

a) A novel paradigm for dynamic and distributed selection of sensing modes in multipurpose IoT devices is introduced. With this feature, the nodes of our setting are able to support various IoT applications that come with specific requirements/parameters set by the infrastructure owner, including sensing accuracy, achievable profit, sensing cost, etc. The dynamic selection functionality is addressed via an adaptive reinforcement learning mechanism.

b) A WPC model is adopted in order to enable the energy efficient operation of the proposed framework. The devices transmit their information during a Wireless Information Transmission (WIT) phase, and the central evolved NodeBase Station (eNB) charges the multipurpose IoT nodes during a Wireless Energy Transfer (WET) phase. The WPC phases occur within the same timeslot where the devices operate in a transmit-harvest-store fashion.

c) A novel coalition formation methodology is proposed, that considers not only the physical parameters, such as the communication/channel conditions between devices and their residual energy availability, but also social related parameters such as possible sensing measurement correlation between devices or their desire for collaboration (e.g., being part of the same IoT application). Our solution operates in a distributed manner towards addressing challenges related to scalability in a dense IoT environment, practical sensing devices' longevity, along with the support of multiple IoT applications that require the collection of diverse or fully/partially correlated data.

d) A distributed resource management mechanism is proposed to optimize the IoT multipurpose devices' energy consumption during the WIT phase. The optimal transmission power vector of the IoT nodes is shown to constitute a unique Nash equilibrium point, and is obtained through a non-cooperative game-theoretic mechanism, that solves the distributed maximization problem of each node's utility function, properly formulated to capture the node's Quality of Service (QoS) prerequisites. To further improve the efficiency of the achieved Nash equilibrium we also consider a convex pricing policy of the devices' uplink transmission power, and utilize an iterative and distributed algorithm to determine the corresponding unique Nash equilibrium.

e) Detailed numerical and comparative results demonstrate that the proposed holistic framework concludes to a promising solution for realizing an energy-efficient IoT environment of multipurpose devices with dynamic behavior, that conforms with the needs and requirements of both the emerging IoT applications and the sensing infrastructure owner.

The rest of the paper is organized as follows. In Section II, the overall system model is described, while in Section III, our proposed reinforcement learning-based mode selection procedure is presented. Section IV introduces the socio-physical ties among the devices and describes the coalition formation process. The energy-efficient uplink transmission power allocation problem is formulated and solved in Section V. Finally,

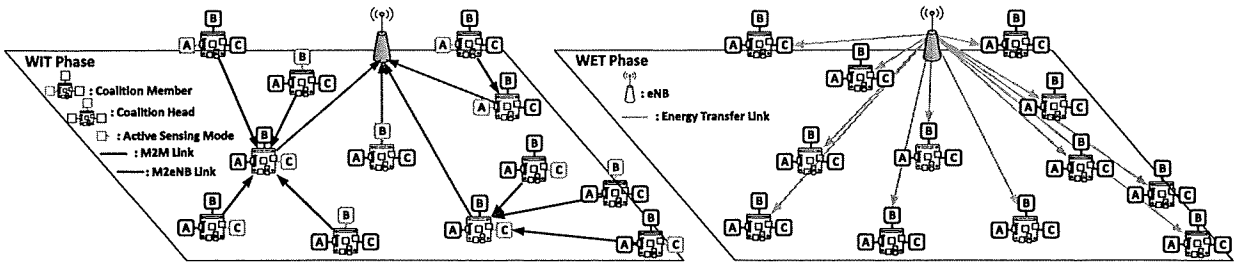

Fig. 1. Network Topology and Operation Phases.

a detailed numerical evaluation of our approach via modeling and simulation is presented in Section VI, while Section VII concludes the paper.

II. System Model

An IoT-inspired sensing infrastructure is considered and modeled as a non-orthogonal multiple access (NOMA) wireless network consisting of an evolved NodeBase Station (eNB) and serving $|M|$ multipurpose IoT devices, where $M = \{1, \ldots, m, \ldots, |M|\}$ denotes their corresponding set. We assume that the devices are identical regarding their characteristics with each one being able to interchange between $|J|$ different sensing modes, e.g., temperature, air quality, building occupancy [23], etc. The set of modes is denoted as $J = \{1, \ldots, j, \ldots, |J|\}$. For the different sensing modes the infrastructure provider defines a specific revenue vector $\mathbf{rev} = [rev_1, \ldots, rev_j, \ldots, rev_{|J|}]$ that stems from the data exploitation and a cost vector $\boldsymbol{c} = [c_1, \ldots, c_j, \ldots, c_{|J|}]$ that derives from the devices' operation. The system topology under consideration is shown in Fig. 1, while system's operation is depicted in Fig. 2. For each timeslot t, the devices select their mode of operation $\boldsymbol{\mu} = \{\mu_1, \ldots, \mu_m, \ldots \mu_{|M|}\}$, $\mu_m \in \{1, \ldots, |J|\}$ following an adaptive reinforcement learning process (Section III). The mode selection process takes into account the provider's revenue/cost relation for each mode, along with socio-physical parameters of the IoT setting itself.

We define two possible communication types: (a) M2M - direct machine to machine communication, (b) M2eNB - where devices communicate directly with the eNB. The devices are able to form $|A|$ coalitions among each other, with the corresponding set denoted as $A = \{1, \ldots, a, \ldots, |A|\}$. Each coalition a selects a coalition head ch_a device, which is in charge of collecting the measurements from the members and forward them to the eNB. The proposed coalition formation considers the energy availability of the devices, their current operating mode, and their given channel quality. The channel gain between two devices is denoted as $G_{m,m'}$, where $m, m' \in M$ while $G_{m,m}$ expresses the channel gain between the device m and the eNB.

The last components of the proposed system and model is the resource allocation and wireless energy harvesting frameworks. Regarding the WPC model [24], we adopt a transmit-harvest-store mechanism assuming that each multipurpose IoT device is equipped with a built-in rechargeable battery. Each timeslot t is divided into two phases, where

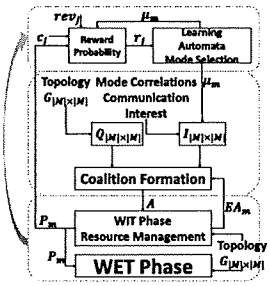

Fig. 2. Proposed framework model - Single timeslot.

initially each node transmits information for time τ_1 (Wireless Information Transmission - WIT phase). Following that, the eNB broadcasts RF-signals in the downlink and each IoT device harvests energy for time τ_2 (Wireless Energy Transfer - WET phase), with $t = \tau_1 + \tau_2$. In order to calculate the optimal uplink transmission power (denoted as P_m^*) of each device, we solve an optimization problem aiming to maximize each device's utility-based perceived satisfaction and meet its Quality of Service (QoS) prerequisites, as detailed later in Section V. The aforementioned described overall procedure is repeated for every timeslot t (Fig. 2).

A. Wireless Channel Model

For our system's operation, we consider a NOMA wireless setting and define the channel gain between a transmitting IoT device m and a receiver m' as:

$$G_{m,m'} = \frac{K}{d_{m,m'}^2} \tag{1}$$

where K represents the shadow effect modeled as a log normal random variable with zero mean and variance of σ^2. Due to NOMA's Successive Interference Cancellation (SIC) technique, at the receiver the messages originated from better channels are decoded first [25]. Assuming that, without loss of generality, the channel gains observed by IoT node m (receiver) are sorted as $G_{|M|,m} \leq \ldots \leq G_{m',m} \leq \ldots \leq G_{1,m}$, the SIC mechanism first decodes the messages received from the best channel, i.e., $G_{1,m}$. Thus, the transmissions of IoT devices with higher channel gain experience interference from the majority of coexisting nodes, while the transmissions of IoT devices with lower channel gain receive less interference by treating the already decoded signals as noise.

Thus, the interference sensed by the m^{th} device is defined as:

$$I_m(\mathbf{P_{-m}}) = \sum_{m' \geq m+1}^{|M|} G_{m',m} P_{m'} + I_0 \quad (2)$$

where I_0 denotes the thermal noise modeled as Additive White Gaussian Noise (AWGN) power, and $\mathbf{P_{-m}}$ is the uplink transmission power vector of the rest IoT devices excluding device m. Finally, the m^{th} node's ($m \in M$) signal-to-interference-plus-noise-ratio (SINR) towards a receiver k is given by:

$$\gamma_m(P_m, \mathbf{P_{-m}}) = \frac{G_{m,k} P_m}{I_k} \quad (3)$$

with I_k being the receiver's sensed interference (Eq. (2)) and P_m the device's uplink transmission power.

III. Socio-Physical Mode Selection

During each timeslot t, the multipurpose devices initially select their operation mode $\mu_m, \forall m \in M$. Each IoT node, acting as a learning automaton, senses the environment and makes the sensing mode selection by relying on its own action history and acquired knowledge from previous timeslots. This is achieved through a two stage reinforcement learning-based process as follows.

A. Reward Probability Formulation

During the first stage our system constructs a reward probability $r_j^{[t]}$ associated with the choice of mode j for the current timeslot, formulated as follows:

$$r_j^{[t]} = \frac{\hat{r}_j^{[t]}}{\sum_{j=1}^{|J|} \hat{r}_j^{[t]}}, \quad \hat{r}_j^{[t]} = \frac{rev_j}{c_j \cdot M_j^{[t-1]} \cdot \frac{\sum_{\forall m:\mu_m=j} P_m^{[t-1]}}{\sum_{m=1}^{|M|} P_m^{[t-1]}}} \quad (4)$$

where $M_j^{[t-1]}$ is the number of devices operating at mode j during the previous timeslot $[t-1]$ with $\sum_{j=1}^{J} M_j = |M|$, $\sum_{\forall m:\mu_m=j} P_m^{[t-1]}$ is the partial power sum of all the devices operating at mode j during the previous timeslot $[t-1]$, and $\sum_{m=1}^{|M|} P_m^{[t-1]}$ is the overall devices' power consumption during the previous timeslot $[t-1]$. Evidently, the reward probability $\hat{r}_j^{[t]}$ reflects the "competitiveness" of each mode j as formed not only by the provider's indications (revenue/cost per mode), but also by the state of the setting during the previous timeslot, e.g., power consumption and devices' distribution per mode.

B. Reinforcement Learning-Based Mode Selection

Given the reward probability $r_j^{[t]}$ we define for each IoT-device/learning automaton $m, m \in M$, an action probability vector $\mathbf{Pr_m^{[t]}} = \{Pr_{m,1}^{[t]}, \ldots, Pr_{m,j}^{[t]}, \ldots Pr_{m,|J|}^{[t]}\}$ where $Pr_{m,j}^{[t]}$ denotes the probability of device m selecting the mode j during the current timeslot. The action probabilities $Pr_{m,j}^{[t]}$ are updated following the learning automata model [26] as follows. For a device operating in mode $\mu_m = j$ the probability of continuing on the same mode j is given by:

$$Pr_{m,j}^{[t]} = Pr_{m,j}^{[t-1]} + b \cdot r_j^{[t-1]} \cdot \left(1 - Pr_{m,j}^{[t-1]}\right) \quad (5)$$

while the probability of changing to a new mode $j' \neq \mu_m$ ($j' \in J, j' \neq j$) is given by:

$$Pr_{m,j'}^{[t]} = Pr_{m,j'}^{[t-1]} - b \cdot r_j^{[t-1]} \cdot Pr_{m,j'}^{[t-1]} \quad (6)$$

For both equations parameter b, $b \in [0,1]$ expresses the procedure's learning speed and controls the convergence of the process. The action probabilities for a single device eventually converge to a specific sensing mode for each IoT device. The final mode distribution after convergence constitutes a cost-efficient state for the infrastructure provider that simultaneously prevents mode extinction, and considers the battery-life of the IoT devices mode-wise. This phenomenon is further studied numerically in detail in Section VI.

IV. Adaptive Coalition Formation

Towards improving the energy efficiency of the M2M communication, the multipurpose devices create coalitions a, $a \in A$ among themselves based on socio-physical criteria, i.e., spatial ties, mode correlations (mode ties), and their energy availability [15], as described below.

1) Spatial Ties: In an attempt to establish energy efficient communication among the devices, their physical location combined with the existing channel conditions among them are considered. To that end, we utilize a symmetric matrix $Q = \{q_{m,m'}\}_{|M|\times|M|}$ indicating the physical proximity and the channel quality between two devices m, $m' \in M$ defined as $q_{m,m'} = \frac{G_{m,m'}}{\max_{\forall m,m' \in M}\{G_{m,m'}\}}$, $q_{m,m'} \in [0,1]$ and $q_{m,m}$ denoting the relation between device m and the eNB. A lower value of $q_{m,m'}$ denotes more distant nodes, while higher values of $q_{m,m'}$ correspond to nodes that are closer to each other. A threshold value q_{thr} is considered prohibiting link creation among distant devices m, $m' \in M$, if $q_{m,m'} < q_{thr}$.

2) Energy Availability: The energy availability is considered to select the coalition head ch_a for every coalition a. The coalition heads are in charge of collecting, processing and transferring a great amount of data compared to the coalition members, thus, they spend an increased amount of power. Therefore, we need to interchange the coalition heads to generate fairness among the multipurpose devices. We denote the energy availability of each device as $E_m, m \in M$. In addition, we define an energy availability indicator as $EA_m = \frac{E_m}{\max_{\forall m' \in M}\{E_{m'}\}}$, where $EA_m \in [0,1]$ expresses the relative energy budget of each multipurpose device.

3) Mode Ties: This relation among IoT-devices is of high practical importance since they may either operate as part of the same IoT application or their sensing modes present practical correlations (e.g., temperature/humidity, space occupancy/motion detection etc.). In order to describe these relations between devices we define a symmetric matrix $I = \{i_{m,m'}\}_{|M|\times|M|}$ where each element $i_{m,m'}$ denotes the mode

Algorithm 1: Formation of Socio-Physical Based Coalitions

Input: $EA_{1\times|M|}$, $Q_{|M|\times|M|}$, $I_{|M|\times|M|}$
Output: Set of coalitions $A = \{1, \ldots, a, \ldots, |A|\}$
Initialization : Entire device set as initial coalition $M' = M$
while $|M'| > 1$ **do**
(a) Coalition head selection for current coalition a
$IF_m = EA_m \sum_{m\in M'} i_{m,m'} q_{m,m'}, \quad \forall m, m' \in M'$
$ch_a = \underset{m\in M'}{argmax}\{IF_m\}$
(b) Infer coalition members
for each m in $M' - \{ch_a\}$ **do**
if $i_{m,ch_a} \geq i_{thr}$
and $q_{m,ch_a} \geq q_{thr}$
and $q_{m,ch_a} \geq q_{m,eNB}$ **then**
$m \in$ coalition a
$M' = M' - \{m\}$
end if
end for
(c) Append created coalition a to coalition set A
end while

correlation among the devices m and m'. At this point we further consider two possible cases regarding the values of I matrix. The first case assumes zero correlation among different modes, therefore two devices will either have correlation equal to one (same operation mode), or zero (different operation mode), i.e., $i^A_{m,m'} \in \{0, 1\}$. The second case assumes non-zero correlations among different device modes and therefore $i^B_{m,m'} \in [0, 1]$ with the correlation between common-mode devices being again one. For both cases the elements residing at the main diagonal $i_{m,m}$ denote the device m-eNB correlation, and will be set equal to one since all the devices have the same interest to communicate with the eNB.

The mode correlation table I is updated for every timeslot (Fig. 2) following the device mode selection changes. Different mode correlations (if exist) are given as input from the infrastructure provider who has the supervision of the sensing data types and their usage. Finally, we define a threshold $i_{thr} \in [0, 1]$ that is used to prevent coalition creation among the devices that exhibit poor mode correlations, i.e., $i_{m,m'} < i_{thr}$. For the zero correlations case, we have $i_{thr} = 1$.

A. Coalition Formation Algorithm

Given a subset of multipurpose devices $M' \subseteq M$ that form a coalition a, we define for each device $m \in M'$ an Importance Factor IF_m such that:

$$IF_m = EA_m \sum_{m\in M'} i_{m,m'} q_{m,m'}, \quad \forall m, m' \in M \tag{7}$$

IF_m considers device's physical proximity with the rest devices ($q_{m,m'}$) along with their mode correlation $i_{m,m'}$ weighted by the device's energy efficiency. Following the IF_m formulation, the coalition head ch_a of a is the one with the highest Importance Factor.

Regarding the number of transmissions that each ch_a performs to transmit the coalition members' data to the eNB, we initially consider it equal to the number of unique modes operating within the coalition. As an enhanced and more representative metric of the aggregation efficiency achieved via the coalition creation, applicable in the case of non-zero correlations among different modes, we further define a Mode-based Aggregation Efficiency (MAE) factor as:

$$MAE = |M'| - \sum_{m\in M'} i_{m,ch_a} \tag{8}$$

where $\lceil MAE \rceil$ denotes the number of ch_a-to-eNB transmissions. We will refer to this as MAE approach as opposed to the aforementioned operation. Algorithm 1 describes in detail the coalition formation process that takes place per timeslot (Fig. 2).

V. Devices Resource Allocation

Given the coalition formation, the following devices' resource allocation framework calculates the optimal transmission power P^*_m of each IoT device in a distributed manner. Due to hardware specifications and physical operation limitations we assume that the feasible powers are upper and lower bounded, i.e., $P^{min}_m \leq P_m \leq P^{max}_m$.

Aiming at supporting all the diverse IoT devices' QoS prerequisites, we adopt the concept of the utility function that represents the device's degree of satisfaction in relation to the expected tradeoff between the achieved bandwidth efficiency and the corresponding energy consumption during a given timeslot. Thus, each IoT device is assumed to adopt a differentiable and continuous utility function U_m with respect to its transmission power P_m, formulated as follows [27]:

$$U_m(P_m) = \frac{W \cdot f_m(\gamma_m)}{P_m} \tag{9}$$

where $f_m(\gamma_m)$ expresses an efficiency function that represents the successful transmission probability between a transmitter m and corresponding receiver, and W denotes the system's bandwidth.

The efficiency function $f_m(\gamma_m)$ is assumed to be continuous, twice differentiable, and increasing with respect to γ_m (Eq. (3)), having a sigmoidal-like shape, such that after a γ^{target}_m point, $f_m(\gamma_m)$ is concave, and below it is convex. Without loss of generality, as widely used in [27] and [28], we also adopt:

$$f_m(\gamma_m) = \left(1 - e^{-A\gamma_m}\right)^Z \tag{10}$$

where A, Z are real valued positive parameters that control the slope of the sigmoidal function [27]. Moreover, by controlling parameters A and Z, f_m becomes flexible enough towards capturing user QoS prerequisites for diverse conditions, use cases, and application-related demands within the considered multipurpose IoT environment.

A. Power Control Game

In our framework, each node aims at maximizing its utility as defined in Eq. (9), through selecting an appropriate strategy for the transmission power. Thus, for each IoT device we formulate the following distributed utility maximization problem:

$$\max_{P_m\in A_m} \; U_m(P_m, \mathbf{P_{-m}}) \quad s.t. \; 0 < P_m \leq P^{Max}_m \tag{11}$$

where $A_m = (0, P_m^{Max}]$ is the strategy space of the multipurpose IoT device m, and $\mathbf{P_{-m}}$ is the transmission power vector of the rest IoT nodes (i.e., excluding device m under consideration).

The utility maximization problem is confronted as a non-cooperative game $G = [M, \{A_m\}, \{U_m\}]$ among the IoT nodes and its solution concludes to an equilibrium for the IoT network, following each node's m individual decision, and given the respective decisions of the rest of the devices. A Nash equilibrium point of the game $G = [M, \{A_m\}, \{U_m\}]$ is a vector of nodes' uplink transmission powers $\mathbf{P^*} = [P_1^*, \ldots, P_m^*, \ldots, P_{|M|}^*]^T \in A$, where the strategy set is denoted as $A = A_1 \times \ldots \times A_m \times \ldots \times A_{|M|}$.

Definition 1: A power vector $\mathbf{P^*} = [P_1^*, \ldots, P_m^*, \ldots, P_{|M|}^*]^T$ in the strategy set $A = A_1 \times \ldots \times A_m \times \ldots \times A_{|M|}$ is a Nash equilibrium of the game $G = [M, \{A_m\}, \{U_m\}]$ if the following condition holds true:

$$U_m\left(P_m^*, \mathbf{P}_{-\mathbf{m}}^*\right) \geq U_m\left(P_m, \mathbf{P}_{-\mathbf{m}}^*\right) \tag{12}$$

for every IoT node m, and $\forall\ P_m^* \in A_m$.

Theorem 1: The non-cooperative power control game $G = [M, \{A_m\}, \{U_m\}]$ has a unique Nash equilibrium point $\mathbf{P^*} = [P_1^*, \ldots, P_m^*, \ldots, P_{|M|}^*]^T$, where

$$P_m^*\left(d_{m,m'}\right) = min\left\{\frac{\gamma_m^*\, I_m}{W\, G_{m,m'}}, P_m^{Max}\right\} \tag{13}$$

for all m, $m \in M$, with γ_m^* being the unique positive solution of the equation:

$$\frac{\partial f_m(\gamma_m)}{\partial \gamma_m}\gamma_m - f_m(\gamma_m) = 0 \tag{14}$$

The proof of the above theorem is concluded following similar steps as in the procedure described in [29]. The Nash equilibrium point determined by Eq. (13) can be interpreted as follows: given the strategies of the rest multipurpose IoT nodes, no independent node has the incentive to chose a different strategy, as this would not improve its personal utility. In addition, due to the fact that the Nash equilibrium point exists, the stable outcome of the non-cooperative game G is guaranteed.

B. Power Control Game With Convex Pricing

The distributed decisions taken by selfish players, as described in the previous subsection, do not always drive the system to efficient Nash equilibria. Thus, the application of pricing mechanisms has often been proposed towards obtaining a more socially desirable and improved equilibrium point, that achieves increased operational efficiency [30]. Related approaches introduce a usage-based pricing on each player's uplink transmission power with each device m aiming to maximize an expression of the form $U_m(P_m, \mathbf{P_{-m}}) - c_m(P_m)$, which we will term as net utility U_m^{net}, with U_m being each device's utility and $c_m(P_m)$ a usage-based pricing policy related to the uplink transmission power. Several pricing policies have been considered in the literature towards moving the Nash equilibrium of the system towards a Pareto optimal solution.

Definition 2: A device's power vector $\hat{\mathbf{P}}$ is Pareto optimal if there is no power vector $\mathbf{P}$ such that $U_m(\mathbf{P}) > U_m(\hat{\mathbf{P}})$ for some $m \in M$ and $U_m(\mathbf{P}) \geq U_m(\hat{\mathbf{P}})$, $\forall m \in M$.

Variations of pricing mechanisms include linear pricing [30] with respect to a device's transmission power, or convex pricing [31], [32]. The latter in contrast to the linear approach, considers the fact that the burden of a single player towards the rest of the players, varies for different transmission power ranges. In this work, we adopt a convex pricing mechanism where the infrastructure owner (and thus the eNB) determines the pricing policy and each user's price per resources' usage.

Therefore, based on the above we consider a net utility function of the following form:

$$U_m^{net}(P_m, \mathbf{P_{-m}}) = \frac{W \cdot f_m(\gamma_m)}{P_m} - c_m(P_m), \forall m \in M \tag{15}$$

where $c_m : A_m \rightarrow \mathbb{R}^+$ is a convex pricing function of transmission power P_m for a multipurpose IoT device m. Without loss of generality, we will adopt an exponential pricing function, namely:

$$c_m(P_m) = c \cdot \left(e^{P_m} - 1\right) \tag{16}$$

where $c \in \mathbb{R}$ is a constant positive pricing factor. Thus, for each IoT device the formulated optimization problem can be re-written under the pricing consideration, as follows:

$$\begin{aligned} \max_{P_m \in A_m} \quad & U_m^{net}(P_m, \mathbf{P_{-m}}) \\ & = \max_{P_m \in A_m} \left\{\frac{W \cdot f_m(\gamma_m)}{P_m} - c_m(P_m)\right\} \\ s.t. \quad & 0 < P_m \leq P_m^{Max}, \quad \forall m \in M \end{aligned} \tag{17}$$

The resulting utility maximization problem is also confronted as a non-cooperative game $G_P = [M, \{A_m\}, \{U_m^{net}\}]$ among IoT devices with the net utility function U_m^{net} expressing each node's diverse QoS prerequisites considering the social welfare constrains.

Theorem 2: The non-cooperative game $G_P = [M, \{A_m\}, \{U_m^{net}\}]$, starting from any initial point, converges to a unique Nash equilibrium that is given by $P_{cost}^* \in (0, P_{critical}]$ as:

$$\begin{aligned} P_{cost,m}^* &= min\left\{\min_{\Theta_{k,m}}\left(\operatorname*{argmax}_{\Theta_{k,m}}\left(U_m^{net}(\Theta_{k,m})\right)\right), P_m^{Max}\right\} \\ \Theta_{k,m} &= \left\{P_{1,m}^*, \ldots, P_{K,m}^*\right\},\ for\ k = 1, \ldots, K,\ \forall m \in M \\ & s.t.\ \left.\frac{\partial U_m^{net}(P_m)}{\partial P_m}\right|_{P_m = P_{cost,m}^*} \\ & = 0,\ \left.\frac{\partial^2 U_m^{net}(P_m)}{\partial^2 P_m}\right|_{P_m = P_{cost,m}^*} < 0 \end{aligned} \tag{18}$$

The proof of Theorem 2 follows similar reasoning as in [32] and is omitted for brevity.

In order to calculate the unique Nash equilibrium point P_{cost}^* of the G_P game we utilize a two-part iterative and distributed power control algorithm. The first part is implemented by the eNB that is responsible to collect the IoT device's experienced satisfaction and broadcast back the resulted price.

Algorithm 2: NE for G_P Game - eNB's Part

Output: Optimal pricing factor c_{best}, Final $P^*_{cost,m} \forall m \in M$
Initialization : (I) Set initial pricing factor $c = 0$ and announce it to IoT devices
(II) $\{P^*_{cost,m}(c=0),\ U^{net}_m(c=0)\} \leftarrow$ **Algorithm 3**, $\forall m \in M$
while *not converged* **do**
(a) Increase pricing factor c
$\hat{c} = c + \Delta c$
(b) Each device determines the equilibrium transmission power and computes its net utility
$\{P^*_{cost,m}(\hat{c}),\ U^{net}_m(\hat{c})\} \leftarrow$ **Algorithm 3**, $\forall m \in M$
(c) Check convergence criterion
if $\forall m \in M$: $U^{net}_m(\hat{c}) < U^{net}_m(c)$ **then**
Convergence criterion met, stop **else** $c = \hat{c}$
end if
end while

Algorithm 3: NE for G_P Game - IoT Device's Part

Input: Pricing factor c, Convergence factor e (small value)
Output: $P^*_{cost,m}$, U^{net}_m
Initialization : $i = 0$, Each device $m,m \in M$, transmits with a randomly selected feasible power, i.e., $P^{*\,[i=0]}_{cost,m}$
while *not converged* **do**
(a) Set $i = i + 1$
(b) Given the wireless setting the eNB unicasts each device's sensed interference $I_m(\mathbf{P_{-m}})$, before being used by the IoT device to refine its power $P^{*[i]}_m$ using (18)
(c) Check convergence criterion
if $|P^{*\,[i]}_{cost,m} - P^{*\,[i-1]}_{cost,m}| \leq e$ **then**
Convergence criterion met, stop
end if
end while

The second part is implemented by each node in a distributed fashion, and determines the uplink transmission power following (18). These two algorithms (Algorithm 2, Algorithm 3) constitute a low complexity distributed procedure for each IoT device.

C. Wireless Energy Transfer

Given the derivation of the optimal uplink transmit power for each IoT device during the WIT phase, we determine the charging transmission power P_{eNB} of the eNB during the WET phase as follows:

$$P_{eNB} = min\left\{ \max_{m \in M} \left\{ \frac{\tau_1 \cdot P^*_m}{\tau_2 \cdot n \cdot G_{eNB,m}} \right\}, P^{Max}_{eNB} \right\} \quad (19)$$

For each IoT device m the harvested energy is given by:

$$E^{har}_m = n\, \tau_2\, P_{eNb}\, G_{eNB,m} \quad (20)$$

where $G_{eNB,m}$ is obtained according to Eq. (1) and $n \in (0,1]$ is the energy efficiency conversion factor that depends on the receiver's hardware specifications. We also assume that each device has non-zero initial energy availability when the framework's operation initiates.

VI. Performance Evaluation

In this section, through modeling and simulation, a detailed numerical evaluation of the proposed framework is conducted, in terms of its operation and performance against other approaches. For our evaluation, we considered a wireless NOMA setting that consists of $|M| = 50$ multipurpose devices randomly distributed in a square area of $100m \times 100m$, while an eNB is located at its center. Each device is able to operate at $|J| = 5$ different modes. The thermal background noise is $I_0 = 5 \cdot 10^{-15}$, the system's bandwidth $W = 10^6$ Hz, and the path gain among devices is modeled as $G_{m,m'} = \frac{K}{d^2_{m,m'}}$, where K is the shadow effect modeled as a log normal random variable with mean 0 and variance of $\sigma^2 = 0.25$ dB, and $d_{m,m'}$ denotes the devices' distance. The timeslot's duration is set to $t = 0.5$ *msec*, while it is equally split between the WIT and WET phases. Unless otherwise explicitly stated, we consider the parameter values shown in Table I. In a nutshell our evaluation focuses on the following aspects: (a) properties and operation of the sensing mode selection mechanism, (b) impact of socio-spatial coalition formation on the system's energy efficiency, (c) advantages of the dynamic sensing mode selection process, (d) impact of application and incorporation of pricing policies in the multipurpose nodes' utilities, and (e) the holistic applicability of the proposed framework under different wireless multiple access techniques.

TABLE I
Simulation Parameter Values

Parameter	Description	Value
W	System Bandwidth	10^6 Hz
I_0	AWGN power at the receiver	10^{-15}
i_{thr}	Interest ties' threshold	0.6
q_{thr}	Physical proximity ties' threshold	$2 \cdot 10^{-3}$
b	Learning parameter	0.7
P^{Max}_m	Maximum uplink transmission power	10^{-4} Watt
P^{Max}_{eNB}	Maximum eNB charging power	0.5 Watt
t	Timeslot duration	0.5 *msec*
τ_1	WIT phase duration	0.25 *msec*
τ_2	WET phase duration	0.25 *msec*
n	Energy efficiency conversion factor	0.6

A. Sensing Mode Selection Mechanism Properties

We will first evaluate the sensing mode selection process focusing on the parameters that control the reward probabilities r_j for each mode and the action probabilities Pr_j. We will consider two scenarios regarding the provider's revenue vector **rev**, i.e., scenario A: $\mathbf{rev}^A = [0.8\ 0.6\ 0.4\ 0.2\ 0.1]$ and scenario B: $\mathbf{rev}^B = [0.8\ 0.8\ 0.05\ 0.05\ 0.05]$, while for both of them we utilize the same cost vector $\boldsymbol{c}^A = \boldsymbol{c}^B = [0.1\ 0.1\ 0.1\ 0.1\ 0.1]$ for the provider. Scenario A represents the case where each mode of operation corresponds to different revenue/cost ratio, with the highest ratio assigned to the first sensing mode and the lowest ratio assigned to the last. Using this scenario we first evaluate how parameter b (see Section III) impacts the learning automata mechanism convergence speed towards a unique sensing mode j with probability 1.

Fig. 3 presents the average number of timeslots required so that all devices converge to a final sensing mode, for different values of parameter b. Evidently, higher values of b result to lower convergence time, observing a reduction of 91.35% for $b = 0.9$, when compared to the case of $b = 0.2$. However, it is generally accepted that small values b significantly decrease

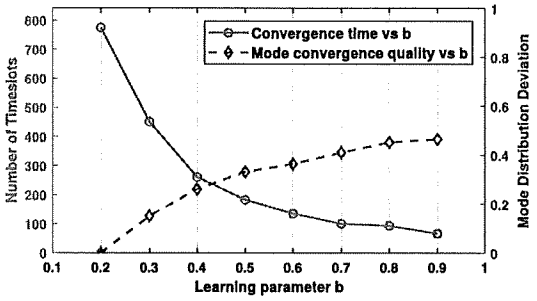

Fig. 3. (a) Average number of timeslots for convergence vs b (b) Mode distribution deviation from the $b = 0.2$ case vs b.

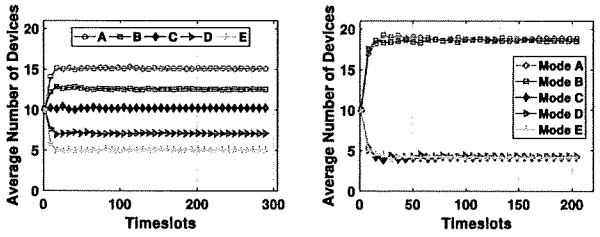

(a) Scenario A (b) Scenario B

Fig. 4. Nodes' distribution per mode (i.e., A, B, C, D, E) as time progresses. (a) Scenario A. (b) Scenario B.

the probability of convergence to the wrong action (here sensing mode selection) [26]. In our case, the reward probability is designed to control the mode distribution among devices towards achieving the provider's revenue/cost requirements and adapt to the IoT environment's needs (prevent sensing mode extinction, and prolong device energy availability). Thus, the complexity of our reward probability does not allow the definition of a convergence mode that is distinctively accurate for each device m. Therefore, in order to evaluate how b affects the mode distribution quality, we calculate the deviation between the mode distribution achieved for the lower b value tested ($b = 0.2$), and the distribution resulted from larger b values as shown by the dashed curve in Fig. 3. For this experiment the network topology remained unchanged for all b values, we utilized a NOMA setting, and the final results were averaged over 500 independent runs. In the remaining of our experimentation, for efficiency and without loss of generality, we use a $b = 0.7$ value, which as shown in Fig. 3, presents a good tradeoff between convergence speed and mode selection quality.

We now focus on the ability of the mode selection learning process to follow the $\frac{\text{rev}}{c}$ ratio that was set by the infrastructure owner towards maximizing his profit. For the two aforementioned scenarios A and B, we averaged the modes distribution per timeslot for 500 individual runs and topologies. As shown in Fig. 4, both scenarios fulfill the $\frac{\text{rev}}{c}$ requirements. Moreover, for scenario B where the two first modes exhibit a significantly larger $\frac{\text{rev}}{c}$ ratio, we observe how the socio-spatial-driven parameters of the reward probability reduce the domination effect of these modes, thus preventing phenomena where modes that present lower revenues are driven to starvation.

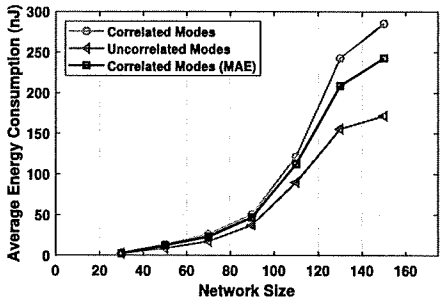

Fig. 5. Average consumed energy vs network size for different modes' correlation scenarios.

B. Impact of Socio-Spatial Coalition Formation

Next, we evaluate how the existence of measurement correlation between devices of different sensing modes (Section IV), impacts the coalition formation quality and the energy consumption of the multipurpose IoT setting considering the NOMA transmission policy (without pricing). The case where there exist sensing mode correlations (e.g., temperature mode and humidity mode) results to coalitions with devices of various modes and therefore, the ch_a is burdened with more transmissions (e.g., as many transmissions as the different modes). On the contrary, when an uncorrelated mode policy is considered ($i_{m,m'} \in \{0, 1\}$) the resulted coalitions consist of identical sensing mode devices that are in the vicinity of the coalition head, who then performs a single transmission to the eNB. However, in order to better and in a more realistic manner reflect the benefit obtained due to the data aggregation, we consider transmission implementation taking into account the MAE factor (Section IV), where the number of ch_a's transmissions per mode drops significantly. Fig. 5 illustrates the average energy consumption for the three modes' correlation settings as network size increases. The results reveal that the uncorrelated mode approach indeed results to lower consumption than the correlated ones, since the latter are associated with the higher number of ch_a to eNB transmissions. The highest energy consumption is observed when the pure correlated mode approach is applied, while under the MAE consideration a consumption in-between the above two approaches is achieved, presenting the tradeoff between energy consumption and the diversity provided by having more than one modes within the same coalition.

By considering non-zero mode correlations for the devices, we additionally discuss how different coalition formation approaches impact the device's average energy consumption. For this purpose we compare four cases as follows:

(a) consider only spatial ties q among devices creating coalitions exclusively between neighboring nodes (q-based).
(b) consider only sensing mode correlations to create coalitions (assuming zero correlations between devices of different sensing modes) (i-based).
(c) apply the proposed socio-physical coalition formation framework under zero correlations among different modes (i-q based).

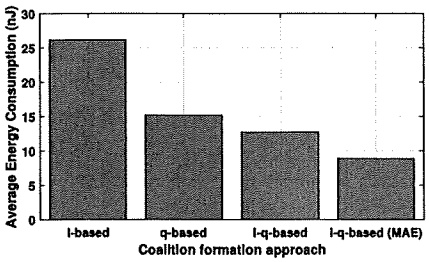

Fig. 6. Average energy consumption per timeslot for different coalition formation scenarios.

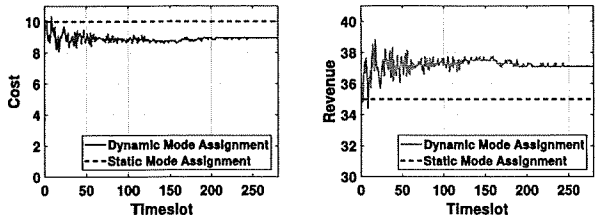

(a) Cost (b) Revenue

Fig. 7. Provider's (a) cost and (b) revenue per timeslot.

(d) same as above under non-zero correlations among different modes and utilizing the MAE driven transmission approach (i-q based MAE approach).

Fig. 6 shows the average energy consumption of the network per timeslot for all the aforementioned alternatives. The q-based method creates coalitions of devices only close to the ch_a with members of various modes, increasing the burden for the ch_a by requiring multiple transmissions towards the eNB. On the other hand, the i-based method creates coalitions relying merely on mode relations and thus ignores spatial distances and channel quality. As a result, the burden is shifted to the member devices that utilize increased transmission power to send their measurements to their ch_a who then report them to the eNB with a single transmission. Evidently, our approach results to better energy consumption compared to the previous two as it achieves a balance between exhausting (energy-wise) either the coalition heads exclusively (q-based case), or the individual members (i-based case). Finally, even lower energy consumption is achieved when considering the MAE factor, since in the latter case coalitions of various modes are formed and at the same time the volume of the *ch*-to-eNB transmissions are reduced.

C. Dynamic Versus Static Sensing Mode Assignment

In this subsection, we examine how the dynamic selection of sensing modes in the multipurpose IoT setting benefits the infrastructure provider in terms of his profit. We assume that the provider has a revenue vector of $\mathbf{rev}' = [0.9 0.8 0.7 0.6 0.5]$, while his initial cost vector is $\mathbf{c}' = [0.1\ 0.15\ 0.2\ 0.25\ 0.3]$. Utilizing these values we calculate the provider's total revenue (Fig. 7b) and total cost (Fig. 7a) per timeslot considering a static assignment of sensing modes uniformly distributed among devices, and compare it against the proposed dynamic mode assignment.

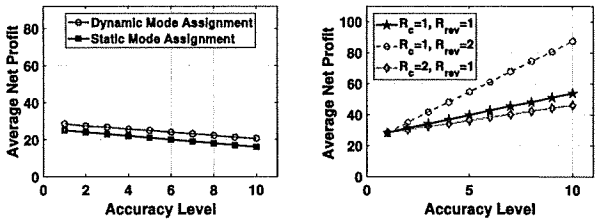

(a) $R_{rev} = 0,\ R_c = 1$ (b) $R_{rev} \neq 0$

Fig. 8. Provider's average net profit for various revenue R_{rev} and cost R_c increase rates.

In addition, we express each multipurpose device's sensing accuracy level using parameter $al \in [1, 10]$ (i.e., 10 setting levels of accuracy, where we assume that a higher value of accuracy leads to higher cost). Considering the cost per mode j for $al = 1$ is $c_j^{[1]} = c'_j$, the accuracy's increase impacts the cost as $c_j^{[al]} = c_j^{[1]} + R_c \cdot \frac{al-1}{10} \cdot c_j^{[1]}$, where R_c denotes the increase rate of cost. Initially, we assume that increased accuracy explicitly impacts the provider's cost with rate $R_c = 1$, while his revenue remains the same, i.e., increase rate of revenue $R_{rev} = 0$, considering the dynamic and static mode assignment cases (Fig. 8a). However, in a realistic scenario by increasing the sensing accuracy the provider's revenue should also increase accordingly, i.e., $rev_j^{[al]} = rev_j^{[1]} + R_{rev} \cdot \frac{al-1}{10} \cdot rev_j^{[1]}$. Fig. 8b depicts the provider's net profit vs accuracy level for three scenarios where (a) revenue and cost increase with the same rate $R_c = R_{rev} = 1$, (b) revenue increases with higher rate ($R_{rev} = 2, R_c = 1$), and (c) cost increases with higher rate ($R_{rev} = 1, R_c = 2$).

D. Impact of Pricing Policies

In this subsection, we focus on the performance of the two distinct WPC phases (i.e., WET and WIT phases) and examine the advantages of adopting uplink transmission power control mechanisms with pricing policies towards more efficient and socially desirable equilibrium points. Specifically, we have examined various wireless network topologies with increasing number of devices across different pricing alternatives focusing on the system's behavior energy-wise. For our comparison we considered the proposed basic NOMA implementation as described before where no pricing mechanism is utilized, against: (a) the use of a linear pricing mechanism in the uplink power control, as discussed in [27], and (b) the use of the convex pricing policy in the uplink power control described in detail in Section V-B. Fig. 9-a shows the energy consumption during the WIT phase as averaged from 500 consecutive timeslots for topologies ranging from 30 to 150 IoT nodes. Evidently, the use of a pricing policy, either linear or convex, leads to lower energy consumption during the WIT phase, since by determining the appropriate choice of pricing policy we manage to improve the system's social welfare towards a more efficient equilibrium for the players with less introduced interference. The reduced performance of the non-cooperative game with no pricing policy is due to its simplified formulation, i.e., the device's adopted utility

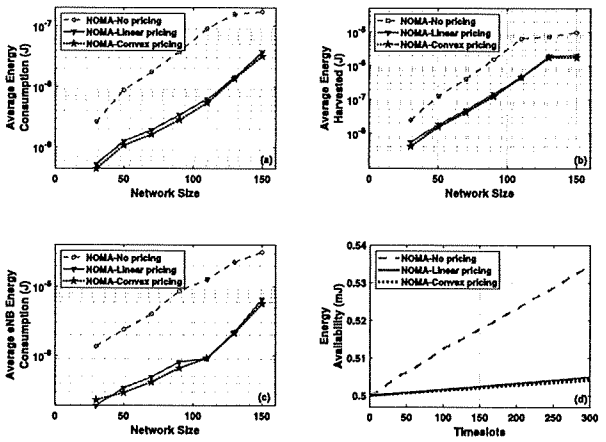

Fig. 9. Pricing Policies' Impact: (a) Average energy consumption in WIT vs network size, (b) Average harvested energy in WET vs network size, (c) Average eNB energy consumption in WET vs network size, (d) System energy availability vs time.

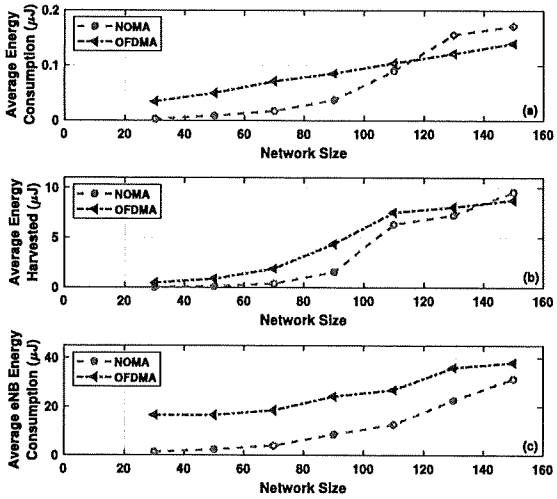

Fig. 10. NOMA versus OFDMA: (a) Average energy consumption in WIT vs network size, (b) Average harvested energy in WET vs network size, (c) Average eNB energy consumption in WET vs network size.

function simply reflects the trade-off between the device's successful transmission probability and corresponding consumed power. In contrast, the introduction of pricing policies creates a non-cooperative game with a utility function that imposes more restrictions with regard to the devices' uplink transmission power levels. In addition, we observe that the proposed convex pricing policy concludes to a more efficient equilibrium for the system, compared to the linear pricing alternative, where the devices use lower uplink transmission powers during WIT.

Examining the performance of the system during the WET phase, we observe that the use of lower WIT phase transmission powers by the devices (e.g., when pricing mechanisms are utilized) leads to lower levels of harvested energy. This is shown in Fig. 9-b where the average harvested system energy over 500 timeslots is shown for topologies ranging from 30 to 150 IoT multipurpose devices. The above result and observation stems from the fact that in our framework the WET phase follows the WIT phase (instead of the opposite order which is commonly encountered in literature). Thus, following Eq. (19) and given the recorded power levels used by the IoT network for the WIT phase, the eNb is able to adjust his charging transmission power P_{eNB} in an attempt to cover the power needs of the devices, while creating in some cases an energy surplus that will be stored. The average eNB consumed energy due to the adjustable charging power is shown in Fig. 9-c for the increasing number of devices. Evidently, the case of no pricing for the uplink power control is a less energy efficient solution when device consumption is considered, while leads to significantly higher values of P_{eNB} for the eNB (and by extension significantly increases the infrastructure provider's costs), when compared to the cases where pricing policies alternatives are assumed. Accordingly, the multipurpose devices operating under no pricing policies show an increased charging rate as shown in Fig. 9-d, that presents the system's total energy availability as time evolves for the scenario of $|M| = 50$ IoT devices.

E. NOMA Versus OFDMA

Finally, in order to demonstrate the holistic applicability of the proposed framework under different wireless multiple access techniques, we have examined an alternative IoT setting that utilizes the Orthogonal Frequency-Division Multiple Access (OFDMA) technique instead. In the OFDMA setting considered, we assume that multiple access is realized by distributing 256 available single frequency channels to the multipurpose IoT devices residing within the range of the sensing infrastructure. In this case, each IoT node experiences a different gain on each available channel. For a single IoT device m that transmits to a receiver k using frequency channel c, the channel gain is defined as: $G_{m,k}^{(c)} = \frac{K \cdot H_c}{d_{m,k}^2}$, where K represents the shadow effect modeled as a lognormal random variable with zero mean and variance of σ^2, while H_c is a random variable expressing frequency channel selective fading. Regarding the channel distribution in an OFDMA environment, algorithms that yield optimal solutions regarding resource allocation are known to be computationally complex [33]. Thus, in order to retain the low complexity nature of our approach, we utilize a greedy sub-optimal allocation method as discussed in [33] and [34], which in principle attempts to allocate channels to users according to the highest channel gain property. Each IoT node's uplink transmission power is calculated by solving a maximization problem of the assigned utility function as found in Eq. (9).

Fig. 10 presents some indicative comparative numerical results of the two implementations (NOMA without pricing and OFDMA), in terms of WIT/WET phase energy characteristics as network size increases. In Fig. 10-a the energy consumption during the WIT phase, averaged over 500 consecutive timeslots, for topologies ranging from 30 to 150 IoT nodes is demonstrated. When sparser topologies are considered the OFDMA implementation leads to higher uplink transmission powers in comparison to NOMA. On the contrary, when

a larger number of IoT devices coexist in our setting (which implements a combination of M2M and M2eNB communications), the small distances between the nodes due to the restricted fixed examination area (small to reflect a practical implementation for indoor spaces) lead to better communication channels, and thus to the more energy-efficient OFDMA performance. However, this enhanced OFDMA performance does not come at no cost, since channel distribution techniques in such environments can be computationally heavy which is a disadvantage in comparison to a NOMA implementation. Considering the system's performance during the WET phase, given the energy requirements for the uplink transmissions, we observe higher average energy consumption by the eNB for charging the IoT nodes under OFDMA, when compared against the NOMA approach. This behaviour is depicted in Fig. 10-c as the number of devices increases. Consequently, higher energy harvesting levels for the devices under OFDMA are observed in Fig. 10-b, where the average system's harvested energy as a function of network size is presented.

VII. Conclusion

In this paper, we studied the orchestration of an energy-efficient operational framework for a set of multipurpose IoT devices capable of making autonomous decisions about their operation in a distributed manner, relying on the awareness of socio-spatial parameters of the surrounding IoT environment. We introduced a reinforcement learning technique towards enabling each IoT node to select a sensing operation mode in accordance with the interests of the IoT infrastructure's provider (e.g., supplying specific measurements to an IoT application, or optimizing his revenue/cost relation). In addition, a coalition formation mechanism of the IoT devices is implemented relying on socio-physical relations among devices, namely spatial distance, energy availability, and sensing mode correlations.

Regarding the information wireless transmission model, we considered a Wireless Powered Communication mechanism where the IoT nodes initially transmit their information, before harvesting energy from transmissions originated by the available eNB. To further improve the overall system energy efficiency, a utility based transmission power allocation approach was introduced, by formulating a power control problem and treating it as a non-cooperative, distributed game among the various IoT nodes. For this uplink power control game we examine two alternatives: (a) a basic one where no pricing for the IoT nodes' utility was used and (b) an enhanced approach adopting a utility with convex pricing, where a cost related to the devices' uplink transmission power is used to obtain a more socially desirable equilibrium point, that was shown to achieve increased operational efficiency.

The operation and performance of our proposed framework were extensively evaluated through modeling and simulation, while the presented detailed numerical results demonstrate its superior energy efficiency, achieved by introducing individual decision making, socio-spatial awareness, and distributed power control in the examined multipurpose IoT setting. Our current and future work contains the testing of the proposed framework in a realistic testbed environment, while the proposed framework will be extended in order to include additional socio-physical parameters, e.g., trust level of the devices, security/privacy preserving characteristics, or wireless communication protocol.

References

[1] J. Ploennigs, A. Ba, and M. Barry, "Materializing the promises of cognitive IoT: How cognitive buildings are shaping the way," *IEEE Internet Things J.*, vol. 5, no. 4, pp. 2367–2374, Aug. 2018.

[2] I. Leontiadis, C. Efstratiou, C. Mascolo, and J. Crowcroft, "SenShare: Transforming sensor networks into multi-application sensing infrastructures," in *Proc. Eur. Conf. Wireless Sensor Netw.*, 2012, pp. 65–81.

[3] Q. Chi, H. Yan, C. Zhang, Z. Pang, and L. Da Xu, "A reconfigurable smart sensor interface for industrial WSN in IoT environment," *IEEE Trans. Ind. Informat.*, vol. 10, no. 2, pp. 1417–1425, May 2014.

[4] M. Hayashikoshi *et al.*, "Low-power multi-sensor system with power management and nonvolatile memory access control for IoT applications," *IEEE Trans. Multi-Scale Comput. Syst.*, to be published, doi: 10.1109/TMSCS.2018.2827388.

[5] *Samsung Smartthings Multipurpose Sensor.* Accessed: Oct. 13, 2017. [Online]. Available: https://www.smartthings.com

[6] J. Steffan, L. Fiege, M. Cilia, and A. Buchmann, "Towards multipurpose wireless sensor networks," in *Proc. IEEE Syst. Commun.*, 2005, pp. 336–341.

[7] I. Khan *et al.*, "Wireless sensor network virtualization: A survey," *IEEE Commun. Surveys Tuts.*, vol. 18, no. 1, pp. 553–576, 1st Quart., 2016.

[8] L. Sarakis, T. Zahariadis, H.-C. Leligou, and M. Dohler, "A framework for service provisioning in virtual sensor networks," *EURASIP J. Wireless Commun. Netw.*, vol. 135, no. 1, p. 135, 2012.

[9] O. Bello and S. Zeadally, "Intelligent device-to-device communication in the Internet of Things," *IEEE Syst. J.*, vol. 10, no. 3, pp. 1172–1182, Sep. 2016.

[10] N. Kaur and S. K. Sood, "An energy-efficient architecture for the Internet of Things (IoT)," *IEEE Syst. J.*, vol. 11, no. 2, pp. 796–805, Jun. 2017.

[11] Ö. U. Akgül and B. Canberk, "Self-organized things (SoT): An energy efficient next generation network management," *Comput. Commun.*, vol. 74, pp. 52–62, Jan. 2016.

[12] F. Leens, "An introduction to i^2c and SPI protocols," *IEEE Instrum. Meas. Mag.*, vol. 12, no. 1, pp. 8–13, Feb. 2009.

[13] F. K. Shaikh, S. Zeadally, and E. Exposito, "Enabling technologies for green Internet of Things," *IEEE Syst. J.*, vol. 11, no. 2, pp. 983–994, Jun. 2017.

[14] S. Bi, Y. Zeng, and R. Zhang, "Wireless powered communication networks: An overview," *IEEE Wireless Commun.*, vol. 23, no. 2, pp. 10–18, Apr. 2016.

[15] E. E. Tsiropoulou, S. T. Paruchuri, and J. S. Baras, "Interest, energy, and physical-aware coalition formation and resource allocation in smart IoT applications," in *Proc. IEEE 51st Annu. Conf. Inf. Sci. Syst. (CISS)*, Baltimore, MD, USA, 2017, pp. 1–6.

[16] E. E. Tsiropoulou, P. Vamvakas, and S. Papavassiliou, "Joint customized price and power control for energy-efficient multi-service wireless networks via *s*-modular theory," *IEEE Trans. Green Commun. Netw.*, vol. 1, no. 1, pp. 17–28, Mar. 2017.

[17] T. A. Zewde and M. C. Gursoy, "Noma-based energy-efficient wireless powered communications," *IEEE Trans. Green Commun. Netw.*, vol. 2, no. 3, pp. 679–692, Sep. 2018.

[18] E. E. Tsiropoulou, G. Mitsis, and S. Papavassiliou, "Interest-aware energy collection & resource management in machine to machine communications," *Ad Hoc Netw.*, vol. 68, pp. 48–57, Jan. 2018.

[19] Y. Zhao and W. Song, "Energy-aware incentivized data dissemination via wireless D2D communications with weighted social communities," *IEEE Trans. Green Commun. Netw.*, vol. 2, no. 4, pp. 945–957, Dec. 2018.

[20] Z. Ning, X. Wang, X. Kong, and W. Hou, "A social-aware group formation framework for information diffusion in narrowband Internet of Things," *IEEE Internet Things J.*, vol. 5, no. 3, pp. 1527–1538, Jun. 2018.

[21] H.-Y. Hsieh, T.-C. Juan, Y.-D. Tsai, and H.-C. Huang, "Minimizing radio resource usage for machine-to-machine communications through data-centric clustering," *IEEE Trans. Mobile Comput.*, vol. 15, no. 12, pp. 3072–3086, Dec. 2016.

[22] D. Sikeridis, E. E. Tsiropoulou, M. Devetsikiotis, and S. Papavassiliou, "Socio-physical energy-efficient operation in the Internet of multi-purpose things," in *Proc. IEEE Int. Conf. Commun. (ICC)*, 2018, pp. 1–7.
[23] D. Sikeridis, B. P. Rimal, I. Papapanagiotou, and M. Devetsikiotis, "Unsupervised crowd-assisted learning enabling location-aware facilities," *IEEE Internet Things J.*, to be published, doi: 10.1109/JIOT.2018.2810808.
[24] S. Bi, C. K. Ho, and R. Zhang, "Wireless powered communication: Opportunities and challenges," *IEEE Commun. Mag.*, vol. 53, no. 4, pp. 117–125, Apr. 2015.
[25] S. M. R. Islam, N. Avazov, O. A. Dobre, and K.-S. Kwak, "Power-domain non-orthogonal multiple access (NOMA) in 5G systems: Potentials and challenges," *IEEE Commun. Surveys Tuts.*, vol. 19, no. 2, pp. 721–742, 2nd Quart., 2017.
[26] K. S. Narendra and M. A. L. Thathachar, "Learning automata—A survey," *IEEE Trans. Syst., Man, Cybern., Syst.*, vol. SMC-4, no. 4, pp. 323–334, Jul. 1974.
[27] C. U. Saraydar, N. B. Mandayam, and D. J. Goodman, "Efficient power control via pricing in wireless data networks," *IEEE Trans. Commun.*, vol. 50, no. 2, pp. 291–303, Feb. 2002.
[28] J.-W. Lee, R. R. Mazumdar, and N. B. Shroff, "Joint resource allocation and base-station assignment for the downlink in CDMA networks," *IEEE/ACM Trans. Netw.*, vol. 14, no. 1, pp. 1–14, Feb. 2006.
[29] E. E. Tsiropoulou, P. Vamvakas, and S. Papavassiliou, "Supermodular game-based distributed joint uplink power and rate allocation in two-tier femtocell networks," *IEEE Trans. Mobile Comput.*, vol. 16, no. 9, pp. 2656–2667, Sep. 2017.
[30] M. Rasti, A. R. Sharafat, and B. Seyfe, "Pareto-efficient and goal-driven power control in wireless networks: A game-theoretic approach with a novel pricing scheme," *IEEE/ACM Trans. Netw.*, vol. 17, no. 2, pp. 556–569, Apr. 2009.
[31] R. B. Wilson, *Nonlinear Pricing*. New York, NY, USA: Oxford Univ. Press, 1993.
[32] E. E. Tsiropoulou, G. K. Katsinis, and S. Papavassiliou, "Distributed uplink power control in multiservice wireless networks via a game theoretic approach with convex pricing," *IEEE Trans. Parallel Distrib. Syst.*, vol. 23, no. 1, pp. 61–68, Jan. 2012.
[33] I. C. Wong, O. Oteri, and W. McCoy, "Optimal resource allocation in uplink SC-FDMA systems," *IEEE Trans. Wireless Commun.*, vol. 8, no. 5, pp. 2161–2165, May 2009.
[34] J. Lim, H. G. Myung, K. Oh, and D. J. Goodman, "Channel-dependent scheduling of uplink single carrier FDMA systems," in *Proc. IEEE 64th Veh. Technol. Conf. (VTC-Fall)*, 2006, pp. 1–5.

Dimitrios Sikeridis received the Diploma degree in electrical and computer engineering from the University of Patras in 2016. He is currently pursuing the Ph.D. degree with the Department of Electrical and Computer Engineering, University of New Mexico. His main research interests include Internet of Things, M2M/D2D wireless communications, cloud computing, and public safety network architectures.

Eirini Eleni Tsiropoulou received the Diploma degree in electrical and computer engineering, the M.B.A. degree, and the Ph.D. degree in electrical and computer engineering from the National Technical University of Athens, Greece, in 2008, 2010, and 2014, respectively. She was a Post-Doctoral Researcher with the Institute for Systems Research, Department of Electrical and Computer Engineering, University of Maryland from 2016 to 2017, a Visiting Scholar with the University of Texas at Dallas in 2016 for five months, and a Senior Research Associate with the National Technical University of Athens from 2014 to 2015. She is currently an Assistant Professor with the Department of Electrical and Computer Engineering, University of New Mexico. Her main research interests lie in the area of cyber-physical social systems and wireless heterogeneous networks, with emphasis on network modeling and optimization, resource orchestration in interdependent systems, reinforcement learning, game theory, network economics, and Internet of Things. Two of her papers received the Best Paper Award at IEEE WCNC in 2012 and ADHOCNETS in 2015. She was also selected by the IEEE Communication Society—N2Women—as one of the top ten Rising Stars of 2017 in the communications and networking field.

Michael Devetsikiotis (F'12) was born in Thessaloniki, Greece. He received the Diploma degree in electrical engineering from the Aristotle University of Thessaloniki, Greece, in 1988 and the M.S. and Ph.D. degrees in electrical engineering from North Carolina State University, Raleigh, in 1990 and 1993, respectively. In 1993, he joined the Department of Systems and Computer Engineering, Carleton University, Ottawa, ON, Canada, as a Post-Doctoral Fellow, where he became a tenure track Assistant Professor in 1996, and an Associate Professor and the Department Associate Chair in 1998. In 2000, he returned to the Department of Electrical and Computer Engineering with North Carolina State as an Associate Professor, where he became a Professor in 2006. He served as the Coordinator of the Master's of Science in computer networking until 2011, when he became the ECE Director of Graduate Programs, managing one of the largest graduate ECE programs with over 800 students. In 2016, he joined the University of New Mexico as a Professor, and the Chair of the ECE Department with the School of Engineering, University of New Mexico. His research work has resulted in 40 published refereed journal articles, 139 refereed conference papers, and 61 invited presentations, in the area of design and performance evaluation of telecommunication networks, complex socio-technical systems, and smart grid communications. In 2017, he was inducted to the NC State ECE Alumni Hall of Fame. He has served as the Chairman of the IEEE Communications Society Technical Committee Communication Systems Integration and Modeling, and as a member of the IEEE ComSoc Education Board. He has also served as an Associate or Area Editor of several publications of the IEEE and the ACM; and as the technical program committee chair and in other roles for numerous conferences. He served as the Chair of the GITC, the Technical Steering Committee for ICC and Globecom, the flagship conferences of the IEEE Communications Society. In 2016, he was one of the instructors at the 2nd IEEE ComSoc Summer School, Trento, Italy. In 2017, he organized the 3rd IEEE ComSoc Summer School, held at UNM, Albuquerque, NM, USA. From 2008 to 2011, he was an IEEE ComSoc Distinguished Lecturer.

Symeon Papavassiliou received the Diploma degree in electrical engineering from the National Technical University of Athens (NTUA), Greece, in 1990 and the M.Sc. and Ph.D. degrees in electrical engineering from Polytechnic University, Brooklyn, NY, USA, in 1992 and 1995, respectively. He is currently a Professor with the School of Electrical and Computer Engineering, NTUA. From 1995 to 1999, he was a Senior Technical Staff Member with AT&T Laboratories, NJ, USA. In 1999, he joined the Electrical and Computer Engineering Department, New Jersey Institute of Technology, USA, where he was an Associate Professor until 2004. He has an established record of publications in his field of expertise, with over 270 technical journal and conference published papers. His main research interests lie in the area of communication networks, with emphasis on the analysis, optimization, and performance evaluation of mobile and distributed systems, wireless networks, and complex systems. He was a recipient of the Best Paper Award in IEEE INFOCOM'94, the AT&T Division Recognition and Achievement Award in 1997, the U.S. National Science Foundation Career Award in 2003, the Best Paper Award in IEEE WCNC 2012, the Excellence in Research Grant in Greece in 2012, and the Best Paper Awards in ADHOCNETS 2015 and ICT 2016. He also served on the board of the Greek National Regulatory Authority on Telecommunications and Posts from 2006 to 2009.